ELSEVIER

Journal of Alloys and Compounds 296 (2000) 80–86

Journal of ALLOYS AND COMPOUNDS

www.elsevier.com/locate/jallcom

Structural disorder and thermal conductivity of the semiconducting clathrate $Sr_8Ga_{16}Ge_{30}$

B.C. Chakoumakos[a,*], B.C. Sales[a], D.G. Mandrus[a], G.S. Nolas[b]

[a]*Solid State Division, Oak Ridge National Laboratory, P.O. Box 2008, Oak Ridge, TN 37831-6393, USA*
[b]*R&D Division, Marlow Industries, Inc., 10451 Vista Park Rd., Dallas, TX 75238, USA*

Received 7 May 1999; received in revised form 13 July 1999; accepted 13 July 1999

Abstract

The temperature dependence of the atomic displacement parameters for $Sr_8Ga_{16}Ge_{30}$ determined from refinements of neutron powder and single-crystal diffraction data shows that the anomalously large values for one of the two unique Sr atoms persist from 295 to 11 K. Its position is better described by a fractionally occupied four-fold split site, but the rms displacement remains the largest of all of the atoms in the structure. Difference Fourier maps of this Sr site show a residual nuclear density with lobes in the directions of the split-atom positions. The Ga and Ge atoms appear to be fully disordered on the three distinct framework sites. The measured atomic displacement parameters are used to derive estimates of the following thermodynamic related quantities: Debye temperature, 271 K; mean velocity of sound, 2600 m/s; temperature of the Einstein ''rattler'', 85 K; mean free path of heat-carrying phonons, 5.36 Å; and lattice thermal conductivity, 0.008 W/cm-K. © 2000 Elsevier Science S.A. All rights reserved.

Keywords: Atomic displacement parameters; Semiconductor clathrate; Neutron diffraction; $Sr_8Ga_{16}Ge_{30}$

1. Introduction

New directions in the research of thermoelectric materials [1–5] include the clathrate-type compounds of the Group IV elements [6], with the structural formula X_8E_{46} with E=Si, Ge, Sn, Al, Ga, In; X=Na, K, Rb, Cs, Sr, Ba [7,8]. These compounds are cubic, space group *Pm3̄n*, and are isotypic with the type I hydrate structure $X_8(H_2O)_{46}$ of the ice clathrates (Fig. 1) [9]. *Pearson's Handbook of Crystallographic Data for Intermetallic Phases* [10] gives a sparse list of 22 compounds with this structure type, yet a great many more are possible given the ternary and quaternary combinations. More recently, X-ray structural refinements of a number of ternary alkali metal and barium clathrates of this type and related ones have been reported; see, for example, Refs. [11–13] and references therein. The properties that make these materials promising thermoelectric candidates include n-type semiconducting behavior, relatively high Seebeck coefficients and electrical

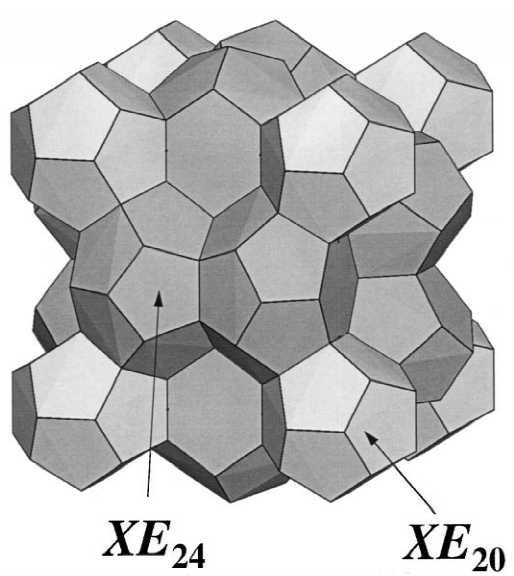

Fig. 1. Space-filling polyhedra of the type I hydrate clathrate structure adopted by the Group IV elements. The crystal data are space group *Pm3̄n* with the structural formula $X_8E_6E_{10}E_{30}$, where E=Si, Ge, Sn, Al, Ga, In; X=Na, K, Rb, Cs, Sr, Ba.

*Corresponding author. Tel.: +1-423-574-5235.
E-mail address: kou@ornl.gov (B.C. Chakoumakos)

0925-8388/00/$ – see front matter © 2000 Elsevier Science S.A. All rights reserved.
PII: S0925-8388(99)00531-9

conductivity, and glass-like thermal conductivity [7]. Here we explore the well-known and anomalously large ''rattling'' of the guest atom in the oversize XE_{24} cage by means of neutron crystallography, and illustrate the use of the atomic displacement parameters to estimate thermodynamically related properties for evaluating thermoelectric behavior.

2. Experimental

For the powder sample synthesis, stoichiometric quantities of high purity constituent elements were mixed and reacted in a pyrolitic boron nitride (BN) crucible for 3 days at 950°C, then annealed at 700°C for 4 days. The BN crucibles were themselves sealed inside a fused quartz ampoule which was evacuated and backfilled with argon gas to a pressure of 0.068 MPa. The ingots were composed of crystallites with dimensions of 1–3 mm^3. These were then ground using an alumina mortar and pestle.

For the single-crystal growth, initially, high purity Sr (99.95%) and Ge (99.9999) were arc-melted together in an argon atmosphere to form nominal $SrGe_2$. The exact composition was determined by weighing the sample before and after melting and assuming the weight loss was due to Sr. Stoichiometric amounts of $SrGe_2$, Ga shot (99.999%) and Ge were loaded in a helium dry box into a carbonized silica tube. $SrGe_2$ was used instead of the elements to prevent reaction of the Sr with the silica tube, and thereby eliminate the need for tantalum capsules. The tube was sealed under high vacuum, placed in a furnace and heated to 1050°C at 2°C/min, held at 1050°C for 20 h and then cooled slowly (0.02–0.1°C/h) to 650°C, held for several days, followed by furnace cooling to room temperature. The resulting boule consisted of large (5–10 mm) single-crystal grains of $Sr_8Ga_{16}Ge_{30}$. Several single crystals of the appropriate size (typically $2\times2\times2$ mm^3) were removed for structure refinement using neutron diffraction.

Neutron diffraction data were collected using the HB-4 high-resolution powder diffractometer at the High-Flux Isotope Reactor (HFIR) at Oak Ridge National Laboratory. With a monochromator $2\theta = 87°$, a Ge 115 reflection was used to give neutrons with a wavelength of 1.5001(1) Å, calibrated with a Si standard. Soller slit collimators of 12′ and 20′ are positioned before and after the monochromator crystal, respectively. An array of 32 nearly equally spaced (2.7°) ^{3}He detectors, each with a 6′ Mylar foil collimator, was step-scanned (0.05°) over a range of 40° for scattering angles between 11 and 135°. The sample was sealed in a vanadium can (13 mm I.D. by 5 cm) with He exchange gas for data collection from 10 to 295 K using a closed-cycle He refrigerator. For these data collections, the detector array was scanned in two segments to overlap up to four detectors in the middle of the pattern. Overlapping detectors for a given step serves to average the counting efficiency and the 2Θ zero-point shift for each detector. Input for the Rietveld refinement program was prepared by interpolating a constant step-size data set from the raw data, because the spacing between the detectors is not exactly the same. The data were also corrected for the variation in detector counting efficiencies, which were determined using a vanadium standard.

Structure refinements were made by the Rietveld method using the GSAS software [14]. The pseudo-Voigt peak-profile function truncated at 0.3% of the peak height was used, including six terms. The background was defined by a cosine Fourier series with three terms. The coherent scattering lengths used were: Sr (7.02 fm), Ge (8.19 fm), and Ga (7.29 fm) [15].

Single-crystal neutron diffraction data were also collected at 295, 230, 155, 85, and 15 K using the HB2a four-circle diffractometer at the HFIR. The 331 reflection from a Ge monochromator at a take-off angle of 45° was used, which gives the neutron wavelength of 1.0037(2) Å for this instrument configuration. A sawn parallelepiped, $1.5\times1.5\times1.75$ mm^3 in size, was glued to an aluminum pin and mounted on the cold-tip of a closed-cycle He refrigerator, which is mounted on the diffractometer and used to control the temperature. For data collection at each temperature the same set of 22 reflections was used for refining the lattice parameter and determining the orientation matrix. The data collections were carried out by radially scanning through the Ewald sphere. At the limits of $2\Theta = 0$ and 180° the radial scan is a pure ω scan and a pure Θ–2Θ scan, respectively; and in between a simple trigonometric relationship controls the relative speeds of the ω and 2Θ motors. A 1/8 sphere of Bragg reflections was measured with $k \geq h$ to $\sin\Theta/\lambda = 0.763$ $Å^{-1}$. Three reflections were monitored to correct the intensities for variations in the neutron flux, which did not vary by more than 1% for the duration of each data collection. The reflection intensities were integrated using the Lehmann–Larson algorithm and corrected for the Lorentz effect with the UCLA Crystallographic Software [16]. The linear neutron attenuation factor, including both incoherent scattering and absorption, for the crystal used in this study is small, 0.0612 cm^{-1}. The intensities of equivalent reflections were averaged in the cubic space group $Pm\bar{3}n$. For each temperature, approximately 1200 reflections were measured, leading to about 200 independent reflections with $F_{obs}/(\sigma F) > 3$, and a data-to-parameter ratio >11. Observed structure factors were used in least-squares refinement of the scale factor, atom positional parameters, and anisotropic atomic displacement parameters. Becker–Coppens type I extinction correction was refined. An isotropic displacement parameter was used for the Sr2 site in the split-site model, and Table 1 summarizes these refinement results. Anisotropic atomic displacement parameters can be obtained from the authors upon request.

Table 1
Rietveld refinement results for $Sr_8Ga_{16}Ge_{30}$, $Pm\bar{3}n$, $Z = 1$, 24j split-site model from neutron powder diffraction data[a]

Temp. (K)	11	60	120	180	240	295
Cell a (Å)	10.69839(8)	10.69994(8)	10.70437(8)	10.71060(9)	10.71710(9)	10.72365(9)
$\rho_{calc.}$ (g/cm^3)	5.417	5.414	5.407	5.398	5.388	5.378
R_p	0.0587	0.0604	0.0586	0.0604	0.0596	0.0548
wR_p	0.0730	0.0750	0.0731	0.0741	0.0748	0.0686
χ^2	1.418	1.495	1.416	1.456	1.489	1.582
U(Sr1) (Å^2)	0.0039(9)	0.0050(9)	0.008(1)	0.011(1)	0.013(1)	0.015(1)
U(Sr2) (Å^2)	0.010(1)	0.014(1)	0.016(1)	0.023(2)	0.029(2)	0.032(2)
y(Sr2)	0.4758(2)	0.4759(3)	0.4758(3)	0.4763(3)	0.4764(4)	0.4660(4)
U(M1) (Å^2)	0.0049(4)	0.0061(5)	0.0061(5)	0.0090(5)	0.0110(6)	0.0120(5)
U(M2) (Å^2)	0.0010(2)	0.0019(2)	0.0035(2)	0.0053(3)	0.0073(3)	0.0085(3)
x(M2)	0.18396(7)	0.18409(7)	0.18403(8)	0.18418(8)	0.18418(8)	0.18424(8)
U(M3) (Å^2)	0.0022(2)	0.0026(2)	0.0039(2)	0.0062(2)	0.0077(2)	0.0092(2)
y(M3)	0.30905(9)	0.3091(1)	0.3089(1)	0.3090(1)	0.3089(1)	0.3088(1)
z(M3)	0.11661(9)	0.1167(1)	0.1169(1)	0.1169(1)	0.1168(1)	0.1169(1)

[a] Atom positions: Sr1 2a 0,0,0; Sr2 24j 1/4,y,y + 1/2; M1 6c 1/4,0,1/2; M2 16i x,x,x; M3 24k 0,y,z. Occupations of M1, M2 and M3 are each fixed at 34.78% Ga and 65.21% Ge; Sr2 site is 25% occupied.

3. Results

3.1. Powder diffraction

For the Rietveld refinements, the starting model was taken from the Ba analog reported by Eisenmann et al. [6]. The structure has two distinct sites for the alkaline earth atoms and the cage framework contains three distinct metal sites occupied by Ge and Ga. The distribution of the Ge and Ga over the framework sites cannot be determined using conventional X-ray diffraction data; but for neutron diffraction data, the scattering lengths are sufficiently different (12%), so that various site occupancy models can be tested and compared. Of nine models tested, the fully disordered model, i.e. 34.78% Ga/65.22% Ge on each metal site, gives the best overall fit.

From the initial refinements, the isotropic atomic displacement parameter for Sr2 was enormous, suggesting that a fractionally occupied split-atom site might be more appropriate. Moreover, anisotropic refinement of the displacement parameters indicates a much smaller displacement amplitude in the ⟨100⟩ directions than in the perpendicular directions (Fig. 2a). This suggests that the Sr2 position at 1/4,1/2,0 could also be described by splitting it into four positions within the {100} planes (Fig. 2b). Furthermore, we see no evidence for a superlattice or other indications of lower symmetry, so we can assume the Sr2 atom is disordered over the split-atom position and the average symmetry remains $Pm\bar{3}n$. Within this space group, a four-fold splitting of the Sr2 sites can be accomplished in two ways, using either of the adjacent 24k or 24j Wyckoff sites. Either one gives essentially the same refinement result, but for the 24j positions there is only one additional positional parameter, whereas for the 24k positions there are two. However, the coordination environments for the 24k and 24j sites are somewhat different. For the 24k position (site symmetry m), the near-neighbor M atoms within 3.85 Å number 16 and have a mean distance of 3.679 Å. For the 24j position (site symmetry 2) the coordination number is 12 and the mean Sr2–M distance is 3.619 Å (see Fig. 3a). For the single-site model, i.e. Sr2 at

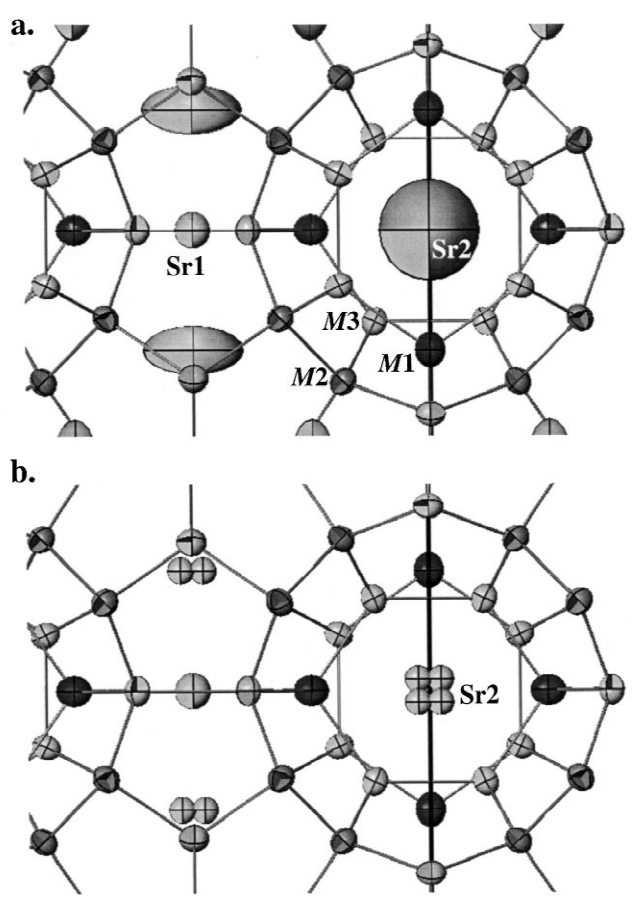

Fig. 2. Crystal structure projection along (100) for $Sr_8Ga_{16}Ge_{30}$ showing the difference in the atomic displacement probability densities for the single site (top) and split site (bottom) of the Sr2 position. Ellipsoids are drawn for 99% probability.

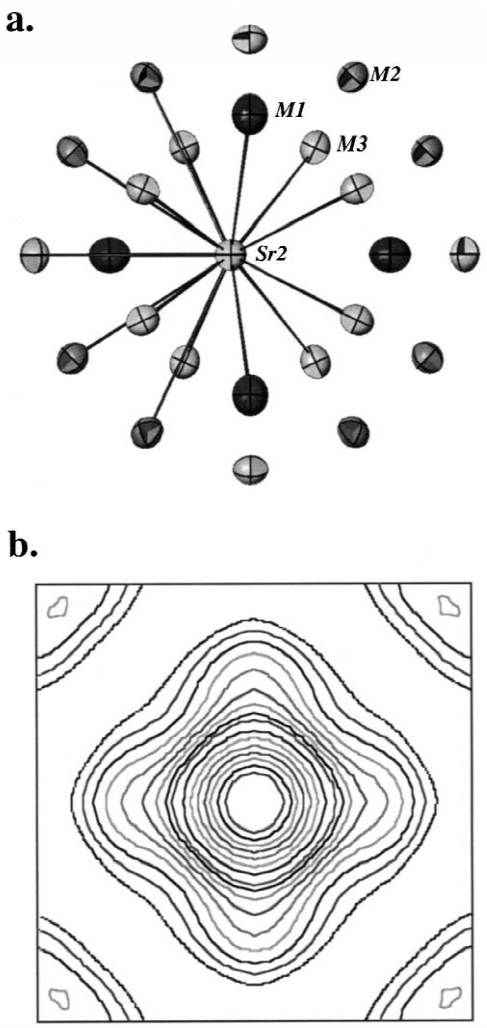

Fig. 3. (a) Sr2 coordination environment projected along (100) of the split-site model using the 24k positions. One of the four equivalent split sites is shown with the near-neighbor distances less than 3.85 Å drawn. The split-site position has mirror symmetry, and the near-neighbor distances less than 3.85 Å number 12 as in the single-site model. The 24j positions are in between the 24k positions. (b) 100 section of the difference Fourier map of the Sr2 site, where the Sr2 atom has been removed from the structural model. The difference nuclear density at the Sr2 site has lobes in the directions of the 24k sites. The map size is 2.5 $Å^2$, and the contour interval is 0.1 $fm/Å^3$ (between 0 and 1.8) and 0.2 $fm/Å^3$ (above 1.8).

the 6d position, the coordination number is 12 and the mean Sr2–M distance is 3.664 Å. Since the mean Sr2–M distance is shortest for the 24j position, it might be energetically more favored. For comparison, the mean Sr1–M distance is 3.494 Å. The minimum separation between near-neighbor Sr2 atoms is 5.36 Å in the single-site model. The Rietveld refinement results are given in Table 1 for the split-atom model using the 24j positions and isotropic displacement parameters.

From the temperature dependence of the isotropic displacement parameters for $Sr_8Ga_{16}Ge_{30}$ (Fig. 4) the apparent $U(T)$ is enormous for Sr2 in the single-site model, and would imply a very large positional disorder by the low-temperature intercept. With Sr2 fractionally occupying a split site, its ADP value is dramatically reduced, but still remains the largest of all the atoms in the crystal. Splitting the site essentially removes a good portion of the positional disorder, since the $U(T)$ curves are essentially parallel for both models. Unconstrained refinement of the Sr2 site occupancy indicates no deficiency at the Sr2 position for either model. The ADP for the Sr1 site is also large, but more on a par with the Ga,Ge sites due to its smaller sized coordination environment.

3.2. Single-crystal diffraction

The single-crystal refinements yield results close to those of the Rietveld refinements, and although the precision is not as good (Table 2), the estimated uncertainties are expected to be more reasonable. For the single-crystal refinements it was not possible to test site occupancy models further for the Ge and Ga distribution among the metal sites, so the occupancies were fixed at the values for the random distribution. Initially, refinements were made with the Sr2 single-site model. These showed the mean square displacements of Sr2 to be extremely anisotropic, $\langle u_1 \rangle = 0.024(5)$ $Å^2$ and $\langle u_3 \rangle = 0.123(9)$ $Å^2$, at room temperature, where the minimum displacement is in the [100] direction and the maximum is in the perpendicular directions. Moreover, difference Fourier maps of the Sr2 site, for which the Sr2 atom was removed from the structural model, clearly show the residual nuclear density to have lobes in the directions of the 24k split-site positions (Fig. 3b). When refinements are carried out with this split-site model, the refined Sr2 atom position is about 0.3 Å away from the single-site 1/4,1/2,0 position in the ***y***-direction. Note that the refinements of the single-crystal neutron diffraction data using the split-site model have about the same agreement as refinements using the single-site model.

4. Discussion

The framework atom positions do not show any temperature dependence which is consistent with the framework being stiff. The thermal linear contraction of $Sr_8Ga_{16}Ge_{30}$ is larger than Ge metal (Fig. 5) as one might expect, because of its lower melting point, 770°C. The contraction of the sample used for the single-crystal measurement is slightly greater than that of the powder sample (Fig. 5), which suggests that the single crystal is slightly more enriched in Ga than given by the nominal composition. The M–M distances in $Sr_8Ga_{16}Ge_{30}$, M1–M3 2.497(1) Å, M2–M2 2.442(3) Å, M2–M3 2.492(1) Å, and M3–M3 2.507(2) Å, are generally slightly longer than the metal–metal distances in germanium (2.450 Å) and gallium (2.440 Å). Note that the densities of Ge (5.323

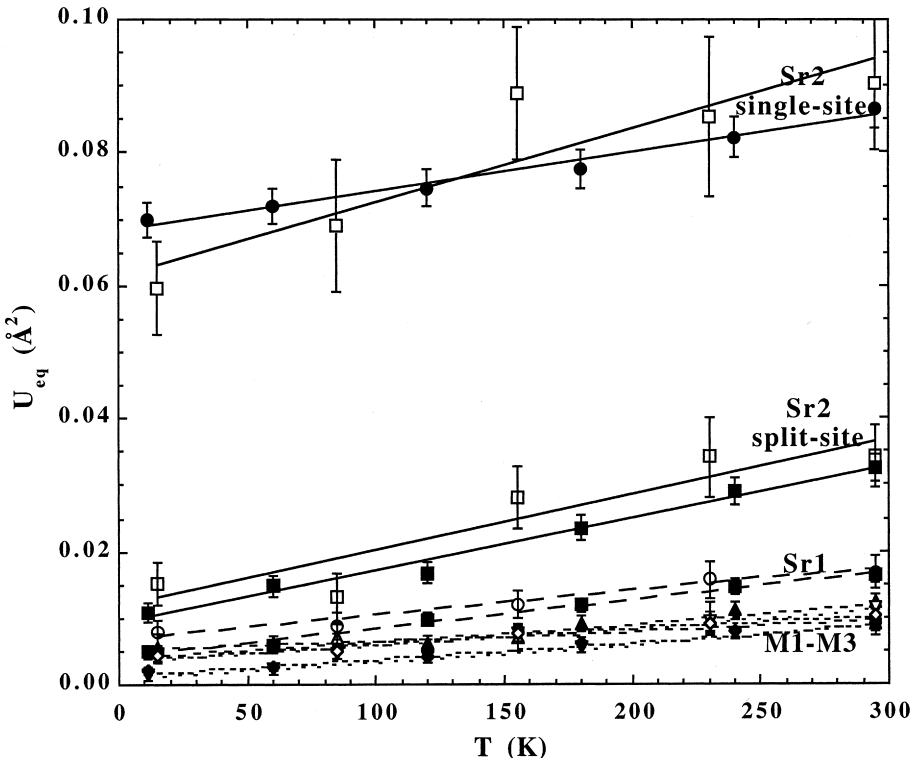

Fig. 4. Temperature dependence of the isotropic displacement parameters for $Sr_8Ga_{16}Ge_{30}$. The apparent $U(T)$ is enormous for Sr2 in the single-site model, and would imply a large static disorder by the low-temperature intercept. Open symbols, single-crystal measurements; solid symbols, powder measurements.

g/cm^3), Ga (5.904 g/cm^3) and $Sr_8Ga_{16}Ge_{30}$ (5.378 g/cm^3) are similar.

Previously [5], we have shown how the high-temperature slope of the $U(T)$ data, $3h^2/(mk_B\theta_D^2 4\pi^2)$, can be used to estimate the Debye temperature. First, either the room temperature U values or the slopes of $U(T)$ are used to calculate a weighted average value. The average atomic mass is used for m, and the ''rattling'' atom is excluded. Given the Debye temperature, the average velocity of sound can be estimated by $v_s = (\theta_D k_B 2\pi/h)/(6\pi^2 n)^{1/3}$,

Table 2
Refinement results for $Sr_8Ga_{16}Ge_{30}$, $Pm\bar{3}n$, $Z = 1$, 24k split-site model from neutron single-crystal diffraction data[a]

Temperature (K)	15	85	155	230	295
Measured reflections	1238	1238	1238	1184	1240
Independent reflections	442	442	442	442	443
Reflections with $I > 3\sigma(I)$	242	225	221	205	202
$R(F)$	0.065	0.075	0.063	0.075	0.054
$wR(F^2)$	0.113	0.124	0.111	0.131	0.101
Goodness of fit, S	1.859	1.719	1.588	1.631	1.387
Extinction coefficient	0.00021(1)	0.00023(2)	0.00025(1)	0.00027(2)	0.00029(2)
Cell a (Å)	10.708(2)	10.715(2)	10.723(2)	10.734(2)	10.743(1)
$\rho_{calc.}$ (g/cm^3)	5.402	5.391	5.379	5.363	5.349
U_{eq} (Sr1) (Å^2)	0.008(1)	0.006(1)	0.011(1)	0.016(2)	0.014(1)
U_{eq} (Sr2) (Å^2)	0.015(3)	0.013(3)	0.028(4)	0.034(5)	0.034(4)
y(Sr2)	0.248(2)	0.251(2)	0.254(2)	0.247(3)	0.251(2)
z(Sr2)	0.529(1)	0.533(1)	0.532(1)	0.532(1)	0.533(1)
U_{eq} (M1) (Å^2)	0.0057(1)	0.0052(1)	0.0084(1)	0.0097(2)	0.012(1)
U_{eq} (M2) (Å^2)	0.0042(1)	0.0042(1)	0.0071(1)	0.0091(1)	0.010(1)
x(M2)	0.1841(1)	0.1841(1)	0.1840(1)	0.1842(1)	0.1840(1)
U_{eq} (M3) (Å^2)	0.0046(1)	0.0057(1)	0.0075(1)	0.0088(1)	0.010(1)
y(M3)	0.3091(2)	0.3088(2)	0.3094(2)	0.3085(3)	0.3091(2)
z(M3)	0.1167(2)	0.1168(2)	0.1170(2)	0.1168(2)	0.1170(2)

[a] Atom positions: Sr1 2a 0,0,0; Sr2 24k 0,y,z; M1 6c 1/4,0,1/2; M2 16i x,x,x; M3 24k 0,y,z. Occupations of M1, M2 and M3 are each fixed at 34.78% Ga and 65.21% Ge; the split Sr2 site is 25% occupied.

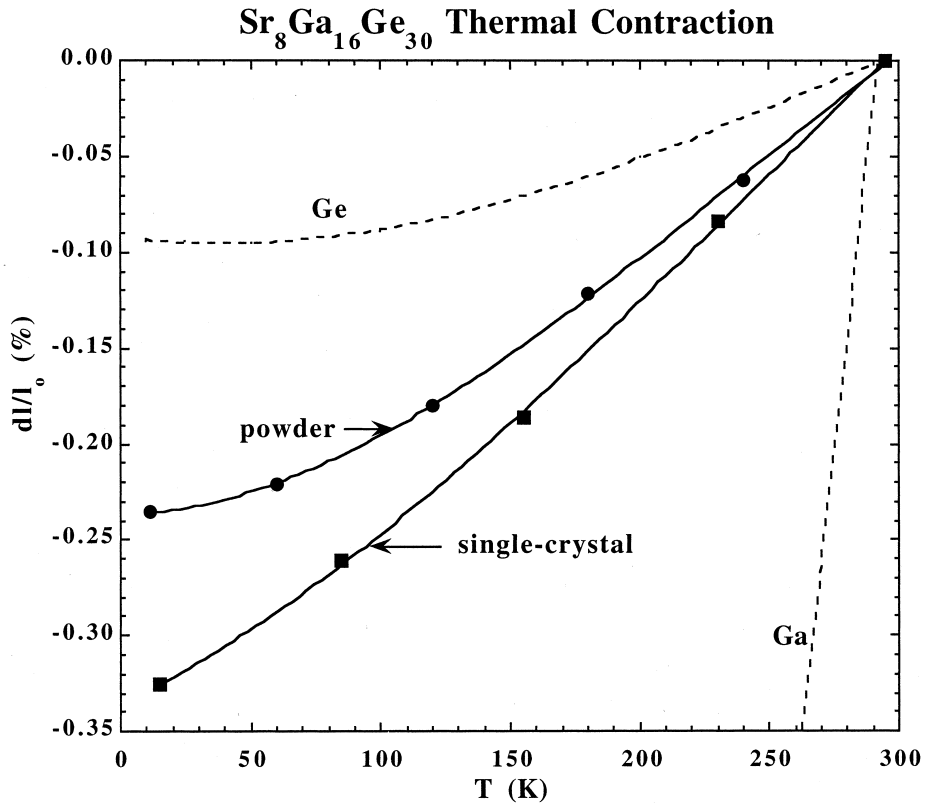

Fig. 5. Thermal linear contraction of $Sr_2Ga_{16}Ge_{30}$, as measured by neutron powder diffraction and single-crystal neutron diffraction, compared with elemental Ge and Ga.

where n is the number of atoms per unit volume. In turn, the lattice thermal conductivity can be estimated by $\kappa_{\text{Lattice}} = 1/3C_v v_s d$, where C_v is the heat capacity per unit volume and d is the mean free path of the phonons. At high temperature, C_v takes on the Dulong–Petit value. Since phonon scattering in materials like this tends to be dominated by the localized vibrations of the ''rattling'' atom [17], then the heat-carrying phonon mean free path should depend on the distance between the ''rattlers''. In $Sr_8Ga_{16}Ge_{30}$ we let d be the minimum separation between near-neighbor Sr2 atoms, or 5.36 Å. The localized vibration of the ''rattler'' may be better described by an Einstein oscillator model, so that $U = k_B T/K$, where $k = m(2\pi\nu)^2$. In this form, the ADP data can be used to estimate the Einstein temperature of the ''rattler''. Table 3 summarizes some of the estimates of the thermodynamic related quantities for $Sr_8Ga_{16}Ge_{30}$. The agreement between the estimated and measured κ_{Lattice} is good.

Table 3
Thermodynamic related quantities for $Sr_8Ga_{16}Ge_{30}$

	Estimates from ADP	Measured
θ_D (K)	271	300[a]
θ_E (K)	85	50[a]
v_s (m/s)	2600	–
d (Å)	5.36	–
κ_{Lattice} (W/cm-K)	0.008	0.009[b]

[a] Unpublished heat capacity data.
[b] From Ref. [7].

What roles do the various forms of structural disorder play in determining the thermodynamic quantities of interest, in particular the lattice thermal conductivity? First, let us enumerate the possible types of structural disorder that are present in these kinds of clathrate compounds. One of the most obvious is the positional disorder associated with either the framework atoms, the ''rattling'' atoms, or both. For this type of disorder the low-temperature intercepts of the atomic displacement parameters determined from the average structure tend to be larger than would be expected from the zero-point motion alone. In principle, this positional disorder can be dynamic or static, but the elastic scattering experiment described here cannot distinguish between these two cases because the time-averaged structures are the same. For clathrate structures where the positional disorder of the caged atoms is extremely large, we can think of the low-temperature intercept of $U(T)$ as being proportional to how flat the potential energy surface is at the ideal position, i.e. center of the caged atom. For extreme cases, such as $Sr_8Ga_{16}Ge_{30}$, the split-site model might not be fictive, since the difference nuclear density at the Sr2 site is not isotropic in all directions. One plausible picture would have the Sr2 atom moving all about the volume enclosed by the probability density

function surface at all temperatures. Clearly, the electrostatic potential within a cage is not the same everywhere, and different points within the cage may be energetically preferred, which suggests that the Sr2 atom might hop or tunnel among the split-site positions. Low-temperature (<1 K) thermal conductivity data indicate the possibility of localized tunnel states in $Sr_8Ga_{16}Ge_{30}$ [18]. Inelastic neutron scattering measurements underway will hopefully elucidate this process.

Another type of structural disorder is due to solid solution, where one or more kinds of atoms are randomly distributed over the same crystallographic sites. A special case of this is when a site is not fully occupied, and vacancies are also randomly distributed over the same site. The disorder associated with the presence of different isotopes of the same elements is generally ubiquitous and not important, except in some special cases, e.g. diamond, where isotopic enrichment can cause significant property changes. When the atomic masses are large, isotopic effects should be small. Last, but not least, there is the thermal motion of the atoms themselves. All of the atomic displacements when analyzed by conventional isotropic or anisotropic refinements assume the quasi-harmonic approximation. Loosely bound caged atoms probably exhibit significant anharmonicity, even at low temperatures. We expect anharmonic effects to be most significant when the harmonic terms are large, as in the case of the Sr2 site in $Sr_8Ga_{16}Ge_{30}$, but because this condition causes the diffraction intensities to dramatically fall off with scattering angle, it becomes more difficult to determine them.

5. Conclusions

1. The atomic displacement parameters for the Sr2 site in $Sr_8Ga_{16}Ge_{30}$ are anomalously large over the entire temperature range, 10 to 300 K, implying a large positional disorder associated with the Sr2 site.
2. The anisotropies of the Sr2 displacements are also large and the site can be equally described by a fractionally occupied four-fold split site, which can effectively account for most of the positional disorder.
3. Difference Fourier maps of the anomalous Sr site show a residual nuclear density with lobes in the directions of the split-atom positions.
4. The Ga and Ge atoms appear to be fully disordered on the three distinct framework sites.
5. The measured atomic displacement parameters allow estimates of the following thermodynamic related quantities: Debye temperature, 271 K; mean velocity of sound, 2600 m/s; temperature of the Einstein ''rattler'', 85 K; mean free path of heat-carrying phonons, 5.36 Å; and lattice thermal conductivity, 0.008 W/cm-K.

Acknowledgements

Oak Ridge National Laboratory is managed by Lockheed Martin Energy Research Corporation for the U.S. Department of Energy under contract number DE-AC05-96OR22464.

References

[1] B.C. Sales, D. Mandrus, R.K. Williams, Science 272 (1966) 1325.
[2] B.C. Sales, D. Mandrus, B.C. Chakoumakos, V. Keppens, J.R. Thompson, Phys. Rev. B 56 (1997) 15081.
[3] G.D. Mahan, B.C. Sales, J. Sharp, Phys. Today March (1997) 42.
[4] B.C. Sales, B.C. Chakoumakos, D. Mandrus, J.W. Sharp, N.R. Dilley, M.B. Maple, in: T.M. Tritt, M.G. Kanatzidis, G. Mahan, H.B. LyonJr. (Eds.), Thermoelectric Materials 1998 — The Next Generation Materials for Small-scale Refrigeration and Power Generation Applications, Materials Research Society Symposium Proceedings, Vol. 545, Materials Research Society, Pittsburgh, 1998, p. 13.
[5] B.C. Sales, B.C. Chakoumakos, D. Mandrus, J.W. Sharp, J. Solid State Chem. (in press).
[6] B. Eisenmann, H. Schäfer, R. Zakler, J. Less-Common Met. 118 (1986) 43.
[7] G.S. Nolas, J.L. Cohn, G.A. Slack, S.B. Schujman, Appl. Phys. Lett. 73 (1998) 178.
[8] G.S. Nolas, in: T.M. Tritt, M.G. Kanatzidis, G. Mahan, H.B. LyonJr. (Eds.), Thermoelectric Materials 1998 — The Next Generation Materials for Small-scale Refrigeration and Power Generation Applications, Materials Research Society Symposium Proceedings, Vol. 545, Materials Research Society, Pittsburgh, 1998, p. 435.
[9] J.S. Kasper, P. Hagenmuller, M. Pouchard, C. Cros, Science 150 (1965) 1713.
[10] P. Villars, L.D. Calvert (Eds.), Pearson's Handbook of Crystallographic Data for Intermetallic Phases, 2nd ed., ASM International, 1991.
[11] R. Kröner, Zintl-Phasen der Alkalimetalle und des Bariums mit Clathratstruktur, Dissertation, Universität Stuttgart, Germany, 1989.
[12] H.G. von Schnering, R.R. Kröner, H. Menke, K. Peters, R. Nesper, Z. Kristallogr. New Cryst. Struct. 213 (1998) 677.
[13] J.-T. Zhao, J.D. Corbett, Inorg. Chem. 33 (1994) 5721.
[14] A.C. Larson, R.B. Von Dreele, Los Alamos National Laboratory Report 1986, LAUR 86-748.
[15] V.F. Sears, Neutron News 3 (1992) 26.
[16] C. Strouse, personal communication.
[17] V. Keppens, D. Mandrus, B.C. Sales, B.C. Chakoumakos, P. Dai, R. Coldea, M.B. Maples, D.A. Gajewski, E.J. Freeman, S. Bennington, Nature 395 (1998) 876.
[18] J.L. Cohn, G.S. Nolas, V. Fessatidis, T.H. Metcalf, G.A. Slack, Phys. Rev. Lett. 82 (1999) 779.